A Supervised Feature-Projection-Based Real-Time EMG Pattern Recognition for Multifunction Myoelectric Hand Control

Jun-Uk Chu, *Member, IEEE*, Inhyuk Moon, *Member, IEEE*, Yun-Jung Lee, *Member, IEEE*, Shin-Ki Kim, and Mu-Seong Mun

***Abstract*—Electromyographic (EMG) pattern recognition is essential for the control of a multifunction myoelectric hand. The main goal of this study was to develop an efficient feature-projection method for EMG pattern recognition. To this end, a linear supervised feature projection is proposed that utilizes a linear discriminant analysis (LDA). First, a wavelet packet transform (WPT) is performed to extract a feature vector from four-channel EMG signals. To dimensionally reduce and cluster the WPT features, an LDA, then, incorporates class information into the learning procedure, and identifies a linear matrix to maximize the class separability for the projected features. Finally, a multilayer perceptron classifies the LDA-reduced features into nine hand motions. To evaluate the performance of the LDA for WPT features, the LDA is compared with three other feature-projection methods. From a visualization and quantitative comparison, it is shown that the LDA produces a better performance for the class separability, plus the LDA-projected features improve the classification accuracy with a short processing time. A real-time pattern-recognition system is then implemented for a multifunction myoelectric hand. Experiments show that the proposed method achieves a 97.4% recognition accuracy, and all processes, including the generation of control commands for the myoelectric hand, are completed within 97 ms. Consequently, these results confirm that the proposed method is applicable to real-time EMG pattern recognition for multifunction myoelectric hand control.**

***Index Terms*—Electromyographic (EMG), linear discriminant analysis (LDA), myoelectric hand control, pattern recognition, wavelet packet transform (WPT).**

I. Introduction

ELECTROMYOGRAPHIC (EMG) signals are used to generate control commands for powered upper limb prostheses. Most commercial myoelectric hands recognize the user's intention by comparing the mean absolute value (MAV) of the EMG signal with a predetermined threshold [1], [2]. This is based on the fact that the amplitude of an EMG signal is almost proportional to the level of muscle activity. However, a simple comparison method using the MAV can only generate a few control commands, such as the opening and grasping of the fingers, or the pronation and supination of the wrist. In recent years, several multifunction myoelectric hands have been developed with a number of DOFs and dexterous hand functions [3]–[5]. Yet, such multifunction myoelectric hands require a robust and computationally efficient EMG pattern-recognition method to classify and control the hand functions. Nonetheless, an EMG signal is essentially a one-dimensional pattern with a large variation and nonstationary properties. In addition, a myoelectric hand system should respond to the user's intention within a short interval, so that the user operates the hand without perceiving a time delay.

Thus, to achieve a high recognition accuracy for multifunction myoelectric hand control, a number of EMG pattern-recognition methods have already been proposed [6]–[8], including a variety of feature-extraction methods for defining a feature vector from the EMG signal, along with various pattern-classification methods for discriminating feature vectors for different classes. The EMG amplitude, zero-crossing rate, histograms, autoregressive coefficients, Fourier transform coefficients, and cepstrum coefficients have all been defined as feature vectors by using a time and frequency analysis [6]–[14]. More recently, time–frequency analysis methods, such as a short-time Fourier transform, wavelet transform (WT), and wavelet packet transform (WPT), have received considerable attention for the analysis of EMG signals [15]–[17]. A time–frequency analysis offers a map of the temporal localization of a signal's spectral characteristics in the time–frequency domain, and yields a high-dimensional feature vector. With the continued increase in the number of motions to be classified, researchers have used multichannel EMG signals and a combination of various feature vectors to increase the information extracted from the EMG signals. That is, feature vectors are expressed with a high dimensionality. For these feature vectors, the classification performance has been investigated by using various classifiers, including a Bayesian classifier [9], [15], [16], Gaussian mixture model [10], [18], hidden Markov model [11], multilayer perceptron (MLP) [6], [8], [13], [17], and fuzzy classifier [7], [12]. However, none of these studies has explained why the classification performance is enhanced, and merely compares the results with those for other methods. Consequently, there is a lack of consideration of the dimension and distribution of the feature vectors extracted from EMG signals. Thus, to analyze the results of feature extraction, a feature-projection method is needed in an EMG pattern-recognition system.

Manuscript received September 1, 2006; revised March 20, 2007. Recommended by Guest Editors H.-P. Huang and F.-T. cheng. This work was supported by the Korea Health 21 R&D Project, Ministry of Health and Welfare, Korea, under Grant 02-PJ3-PG6-EV03-0004.

J. U. Chu and Y. J. Lee are with the School of Electrical Engineering and Computer Science, Kyungpook National University, Daegu 702 701, Korea (e-mail: juchu@ee.knu.ac.kr; yjlee@ee.knu.ac.kr).

I. Moon is with the Department of Mechatronics Engineering, Dong-Eui University, Busan 614 714, Korea (e-mail: ihmoon@deu.ac.kr).

S. K. Kim and M. S. Mun are with the Korea Orthopedics and Rehabilitation Engineering Center, Incheon 403 120, Korea (e-mail: skkim@korec.re.kr; msmun@korec.re.kr).

Digital Object Identifier 10.1109/TMECH.2007.897262

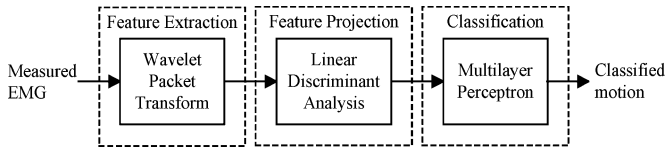

Fig. 1. Block diagram of EMG pattern recognition.

Generally, feature projection can be formulated as a mapping from an original feature space to an appropriate subspace such that a learning criterion is optimized. Feature projection enables high-dimensional feature vectors to be visualized in a low dimension, and allows the distribution of the reduced feature vectors to be analyzed. As a result, the classifier with the best performance can be selected for the reduced feature vectors. Furthermore, if the feature projection is optimized by a learning criterion such that feature vectors belonging to the same class are clustered, the generalization ability of the classifier can be improved. Plus, dimensionality reduction of feature projection reduces the processing time for pattern recognition, and makes real-time implementation possible.

Huang *et al.* [8] defined time-domain feature vectors as histogram and autoregressive coefficients from three-channel EMG signals, and introduced a self-organizing feature map (SOFM) for feature projection. Subsequently, they used an MLP classifier to discriminate eight hand motions. An SOFM is categorized as a nonlinear unsupervised method, as the synaptic weight vectors are adjusted based on their similarity to the input pattern without class information. For this reason, an SOFM sometimes transforms the input patterns for different classes into the same cloud, causing a low accuracy in the classification stage. Meanwhile, Englehart *et al.* [16] extracted WPT coefficients from four-channel EMG signals, and performed dimensionality reduction by using a principal components analysis (PCA). The recognition accuracy for six hand motions was tested by using a Bayesian classifier. The PCA-reduced features were able to approximate the class distribution of the original features, yet the features for different classes were not exactly separated, as the PCA learning merely produced a well-described coordinate system for the distribution of all features, without considering the class separation.

Accordingly, the goal of this study was to develop an efficient feature-projection method for EMG pattern recognition. Thus, to reduce the dimensionality of the features and cluster features while improving the class separability, a linear supervised feature projection is proposed that utilizes a linear discriminant analysis (LDA). The LDA incorporates class information into the learning procedure, and finds a linear matrix to maximize the class separability for the projected features. As a result, a classifier can find a decision surface with an enhanced separation margin, and the classification accuracy is improved. In addition, the linear projection of the LDA allows a short processing time, making real-time implementation possible. Therefore, by using LDA feature projection, the structure of a WPT–LDA–MLP is proposed for EMG pattern recognition, as shown in Fig. 1. To recognize nine kinds of hand motion, the wavelet packet features are first extracted from four-channel EMG signals. The LDA, then, performs the dimensionality reduction and clustering of the WPT features to improve the class separability. In the classification stage, the MLP discriminates the LDA-projected features for different classes. To evaluate the performance of the LDA with WPT features, the LDA is compared with a PCA, nonlinear discriminant analysis (NLDA), and SOFM. For these feature-projection methods, the reduced features are visualized to show the clustering tendency and the class separability are investigated by using Sammon's stress and Fisher's index. The results of the MLP classification success rate and processing time show that the LDA produced the best EMG pattern classification. Finally, a real-time EMG pattern-recognition system is implemented for a multifunction myoelectric hand, and its effectiveness demonstrated.

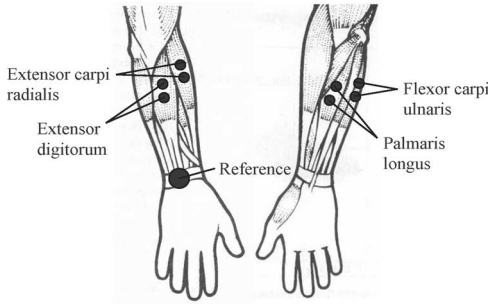

Fig. 2. Surface electrode placement on forearm muscles.

II. Data Acquisition

This study attempted to recognize nine kinds of hand motion: flexion and extension of the wrist, radial and ulnar flexion of the wrist, pronation and supination of the wrist, opening and grasping of the fingers, and relaxation. Since hand motions result from contraction of the muscles in the forearm, four surface electrodes were used to measure the EMG signals from the extensor digitorum, extensor carpi radialis, palmaris longus, and flexor carpi ulnaris, respectively, which are the muscles concerned with hand motions (see Fig. 2).

Generally, the frequency range of an EMG signal is from 0 to 1000 Hz, yet the dominant energy is concentrated between 20 and 500 Hz, and the amplitude is limited from 0 to 10 mV [19]. Therefore, an active surface electrode (DE-2.1, DELSYS) was used, including a bandpass filter with a 10–450-Hz bandwidth, and amplifier with a 60-dB gain. The EMG signals were digitized by using an A/D converter board (6052E, NI), and the sampling frequency was 1024 Hz.

In the experiment, the EMG data were collected from ten normally subjects (seven males and three females, 27 ± 3.3 years.). Twenty sessions were conducted for each subject. The first ten sessions were used for the learning procedures, while the remaining ten sessions were used for the performance evaluations. Each subject was asked to maintain a static contraction for each motion and to change the motions with a fixed movement velocity. In every session, each motion was performed once for a duration of 5 s, then switched to another motion in random order.

The response time of a myoelectric hand control system should be less than 300 ms, so that the user can operate the hand without perceiving a time delay [9]. Thus, a moving window scheme with a window increment is applied to recognize a steady-state motion. Although a small window increment improves the response time of a myoelectric hand, the window increment is determined based on considering the processing time of the pattern-recognition algorithm. For real-time implementation, all processes, including the generation of control commands for the myoelectric hand, must be completed within the window increment. Therefore, in this study, the length of the moving window was set to 250 ms (256 samples) with a 125-ms (128 samples) window increment, thereby allowing the proposed scheme to generate two decisions within 300 ms and guaranteeing user control of directed myoelectric hand functions within 300 ms from the instant the user's intention is given.

III. Algorithm Description

A. Feature Extraction

To extract a feature vector from the EMG signals, a WPT is used that is a generalized version of a wavelet transform. A signal with N points is decomposed into an overcomplete set of subspaces with different time–frequency localization characteristics. The root node $\Omega_{0,0}$ is the original signal space, and a subspace $\Omega_{j,k}$ is decomposed into two orthogonal subspaces $\Omega_{j,k} \rightarrow \Omega_{j+1,2k}$ and $\Omega_{j,k} \rightarrow \Omega_{j+1,2k+1}$, where j denotes the scale and k indicates the subband index within the scale. Each subspace $\Omega_{j,k}$ is spanned by basis vectors $\{w_{j,k,n}\}$, $n = 0, \ldots, 2^{n_0-j} - 1$, where $n_0 = \log_2 N$. This means that the complete basis of the time–frequency plane can take many forms according to the selected partitions of the frequency axis. For the pattern-recognition task, if a proper discriminant measure is introduced, the best basis can be chosen to maximize the class separability specified by the discriminant measure. Thus, in this study, the best basis is determined by using the local discriminant basis (LDB) algorithm proposed by Saito and Coifman [20]. The symmetric relative entropy as a discriminant measure is chosen as

$$D(\mathbf{p}, \mathbf{q}) = \sum_{i=1}^{n} p_i \log \frac{p_i}{q_i} + \sum_{i=1}^{n} q_i \log \frac{q_i}{p_i} \tag{1}$$

where $\mathbf{p} = \{p_i\}$, $\mathbf{q} = \{q_i\}$, $i = 1, \ldots, n$, are the measures used to represent the features from two different classes. For the input parameters to the symmetric relative entropy, the time–frequency energy map for each class is defined as

$$\Gamma_c(j,k,n) = \frac{\sum_{i=1}^{N_c} \left(\mathbf{w}_{j,k,n}^T \mathbf{x}_i^{(c)} \right)^2}{\sum_{i=1}^{N_c} \left\| \mathbf{x}_i^{(c)} \right\|^2} \tag{2}$$

where $j = 0, \ldots, J$, $k = 0, \ldots, 2^j - 1$, and $n = 0, \ldots, 2^{n_0-j} - 1$, plus $\{\mathbf{x}_i^{(c)}\}$, $i = 1, \ldots, N_c$, is the set of training signals belonging to class c, where N_c is the number of patterns in class c. Thus, when combining (1) with (2), the symmetric relative entropy of subspace $\Omega_{j,k}$ for K classes is written as

$$D(\{\Gamma_c(j,k,\bullet)\}_{c=1}^{K}) = \sum_{a=1}^{K-1} \sum_{b=a+1}^{K} D\left(\Gamma_a(j,k,n), \Gamma_b(j,k,n)\right). \tag{3}$$

Let $B_{j,k}$ denote the set of basis vectors belonging to subspace $\Omega_{j,k}$ and let $A_{j,k}$ represent the LDB as the best basis for the candidate set restricted to the span of $B_{j,k}$. For each node (j,k), let $\Delta_{j,k}$ be the symmetric relative entropy. Now, the LDB algorithm can be summarized as follows.

1) Choose a wavelet and scaling function for the WPT, and specify the depth of decomposition J.
2) Construct the energy map Γ_c for $c = 1, \ldots, K$.
3) For the level J, set $A_{j,k} = B_{j,k}$ and $\Delta_{j,k} = D(\{\Gamma_c(J,k,\bullet)\}_{c=1}^{K}), k = 0, \ldots, 2^J - 1$.
4) Determine the best subspace $A_{j,k}, j = J-1, \ldots, 0, k = 0, \ldots, 2^j - 1$, by using the following rule: set $\Delta_{j,k} = D(\{\Gamma_c(j,k,\bullet)\}_{c=1}^{K})$. If $\Delta_{j,k} \geq \Delta_{j+1,2k} + \Delta_{j+1,2k+1}$, then $A_{j,k} = B_{j,k}$, else $A_{j,k} = A_{j+1,2k} + A_{j+1,2k+1}$ and set $\Delta_{j,k} = \Delta_{j+1,2k} + \Delta_{j+1,2k+1}$.

This pruning method performs a local comparison between the parent node (j,k) and the children nodes $\{((j+1,2k),\ (j+1,2k+1)\}$, thereby helping to either keep the parent node or sink deeper toward the children nodes.

In the LDB algorithm, the discrete wavelet decomposition is implemented by using the Mallat algorithm [21], plus the depth of the decomposition level is specified as four, and a Haar wavelet and scaling function are used. To increase the class separability, an LDB is independently constructed for each channel. Thereafter, based on the four LDB sets, the WPT coefficients are obtained, and their absolute values extracted as features in the pattern-recognition procedure. The feature set for each channel is a 256-dimensional feature vector, while the feature set for the four channels is a 1024-dimensional feature vector.

B. Feature Projection

In this study, the EMG pattern recognition is a supervised classification problem in which the training pattern is identified as a member of a predefined class. Therefore, the LDB of the WPT is searched in a supervised manner by using the class information for the segmented EMG signals. The WPT features are, then, applied to a supervised feature-projection method that uses the class information for the learning criterion, such that feature vectors belonging to the same class are clustered. An LDA is, then, adopted as a linear supervised feature-projection method that identifies a linear matrix to make the between-class scatter large and the within-class scatter small [22]. That is, the LDA seeks a coordinate system to maximize the class separability for the projected features.

A linear projection is expressed as $\mathbf{y} = \mathbf{W}^T \mathbf{z}$, where $\mathbf{z}$ is the original feature vector with n dimensionality, $\mathbf{y}$ is the projected feature vector with k dimensionality $(k \leq n)$, and $\mathbf{W}$ is an $n \times k$ matrix. The LDA is mainly based on a family of functions of

scatter matrices. The within-class scatter matrix is defined as

$$\mathbf{S}_W = \sum_{c=1}^{K} \sum_{i=1}^{m} r_i^{(c)} \left(\mathbf{z}_i - \mathbf{m}^{(c)}\right) \left(\mathbf{z}_i - \mathbf{m}^{(c)}\right)^T \quad (4)$$

where $\{\mathbf{z}_i\}, i = 1, \ldots, m$ denote the n-dimensional feature vectors, m is the number of features, $\mathbf{m}^{(c)}$ is the mean vector for class c, and $r_i^{(c)} = 1$ if $\mathbf{z}_i \in c$ and 0 otherwise. Meanwhile, the between-class scatter matrix is defined as

$$\mathbf{S}_B = \sum_{c=1}^{K} N_c \left(\mathbf{m}^{(c)} - \mathbf{m}\right) \left(\mathbf{m}^{(c)} - \mathbf{m}\right)^T \quad (5)$$

where $\mathbf{m}$ is the mean vector for all features. Finally, the total scatter matrix is the covariance for all features, regardless of the class

$$\mathbf{S}_T = \sum_{i=1}^{m} \left(\mathbf{z}_i - \mathbf{m}\right) \left(\mathbf{z}_i - \mathbf{m}\right)^T = \mathbf{S}_W + \mathbf{S}_B. \quad (6)$$

For a scatter matrix, the measure of spread is the determinant. Thus, an $n \times k$ matrix $\mathbf{W}$ is identified that maximizes the learning criterion

$$\frac{\det\left(\mathbf{W}^T \mathbf{S}_B \mathbf{W}\right)}{\det\left(\mathbf{W}^T \mathbf{S}_W \mathbf{W}\right)}. \quad (7)$$

The $n \times k$ matrix $\mathbf{W}$ is composed of k eigenvectors corresponding to the k largest eigenvalues of $\mathbf{S}_W^{-1}\mathbf{S}_B$. Since the matrix $\mathbf{S}_B$ has a maximum rank of $K - 1$, the value of k must be defined as less than K. Therefore, the dimensionality of the projected space is limited by the number of classes. To cope with this limitation, the total scatter matrix is used instead of the between-class scatter matrix in the learning criterion, so that the dimensionality of the projected features is not limited by the number of classes. From this result, the k-dimensional feature $\mathbf{y}$ is obtained.

To determine the dimensionality of the projected feature, the linear dimensionality for 1024-dimensional WPT features extracted from EMG signals was examined. As a result, the linear dimensionality of the WPT features was eight. This means that the ratio of the sum of the eight largest eigenvalues to the sum of the total eigenvalues of the covariance matrix is more than 0.97. Therefore, the WPT features are projected into an eight-dimensional subspace through the LDA.

C. Classification

After the feature projection, the reduced features are given to an MLP classifier. The input layer of the MLP is constructed from the eight outputs of the LDA. The number of hidden layers is two, and each hidden layer has nine neurons. The output layer also has nine neurons for the nine kinds of hand motion to be recognized. This network structure was determined by trial and error. The selection criterion was based on the convergence of the learning error. The input of the MLP was the normalized value of the LDA output, and the initial weights and bias were chosen from a uniform distribution with a mean and variance of 0 and 1, respectively. The learning process was stopped when the absolute rate of change in the average squared error per iteration was sufficiently small. When the LDA-projected features were applied to the MLP, the maximum output of the MLP was selected as the recognized motion.

IV. Performance Evaluation

A. Methodology

For feature-projection methods, the mapping function can be either linear or nonlinear, while the learning procedure can be either a supervised or unsupervised method. In this section, to evaluate the proposed EMG pattern-recognition method, the performance of four methods, including the proposed method, was investigated. The selected methods used an LDA (linear supervised), PCA (linear unsupervised), NLDA (nonlinear supervised), and SOFM (nonlinear unsupervised) for feature projection, respectively. By using these methods, the WPT features were first visualized in a reduced feature space to explore the pattern distribution. For a quantitative comparison of the four projection methods as regards class separability, Sammon's stress and Fisher's index were used. Next, the projected features were applied to an MLP classifier, and the classification performance compared. Finally, the processing times for the four projection methods were evaluated.

A PCA [23] is a linear orthogonal transform where the coordinates of the projected features are uncorrelated, plus the maximum variance of the original features is preserved by a small number of coordinates. First, an $n \times n$ covariance matrix $\mathbf{\Sigma}$ is constructed from the WPT features, and an $n \times k$ matrix $\mathbf{W}$ is formed, where the columns consist of k eigenvectors with the k largest eigenvalues from the covariance matrix. According to $\mathbf{y} = \mathbf{W}^T\mathbf{z}$, the WPT feature vector is, then, projected onto the k-dimensional subspace.

An NLDA [24] is a feature-projection method that involves the nonlinear transformation of an MLP and supervised learning. In an MLP with five layers, the subnetwork from the input layer to the second hidden layer maximizes $\mathrm{Tr}(\mathbf{S}_B\mathbf{S}_T^+)$, where $\mathbf{S}_T^+$ is the pseudoinverse of the total scatter matrix of the features in the second hidden layer and $\mathbf{S}_B$ is the weighted between-class scatter matrix of the features in the second hidden layer. Thus, an MLP is constructed from an n-dimensional input layer, large first hidden layer, k-dimensional second hidden layer (bottleneck), large third hidden layer, and K-dimensional output layer. For the hidden layers and the output layer, a bipolar sigmoid function is used as a nonlinear activation function. Error backpropagation learning is, then, performed on the five-layer MLP by using the WPT features and class information. Thereafter, the third hidden layer and output layer are removed, and the bipolar sigmoid function of the second hidden layer replaced with a linear function. As a result, the NLDA network is composed of the remaining three layers. Finally, the WPT feature vector is transformed into a k-dimensional feature vector through the NLDA network. In this study, the first and third hidden layers had 256 neurons, respectively, which was determined by trial and error to minimize the learning error.

An SOFM [25] basically consists of a two-dimensional lattice of neurons, where each neuron in the lattice is fully connected to all nodes in the input layer. In the learning procedure, the winning neuron $\mathbf{y}(\mathbf{z})$ at time step n is determined by using the

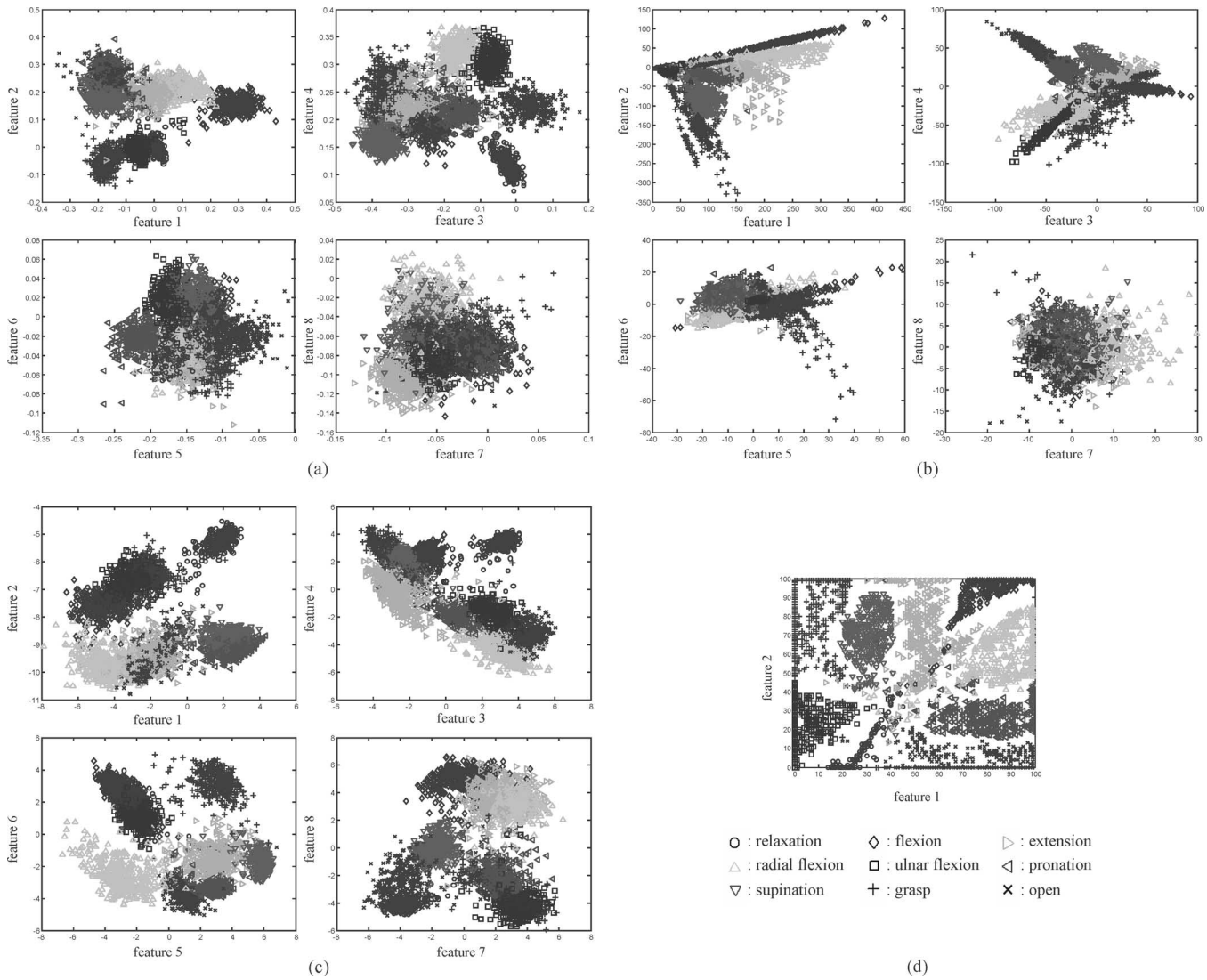

Fig. 3. Dimensionally reduced feature spaces when using (a) LDA, (b) PCA, (c) NLDA, and (d) SOFM.

minimum distance Euclidean criterion

$$\mathbf{y}(\mathbf{z}) = \arg\min_{j} |\mathbf{z}(n) - \mathbf{w}_j(n)|, \quad j = 1, \ldots, l \tag{8}$$

where $\mathbf{w}_j(n)$ represents the weight vectors and l is the number of neurons. The synaptic weight vectors for all the neurons are adjusted by using the update formula

$$\mathbf{w}_j(n+1) = \mathbf{w}_j(n) + \eta(n) h_{j,\mathbf{y}(\mathbf{z})}(n)(\mathbf{z}(n) - \mathbf{w}_j(n)) \tag{9}$$

where the neighborhood function centered on the winning neuron is $h_{j,\mathbf{y}(\mathbf{z})} = \exp\left(-d^2_{j,\mathbf{y}(\mathbf{z})}/2\sigma^2(n)\right), d_{j,\mathbf{y}(\mathbf{z})}$ is the distance between the winning neuron $\mathbf{y}(\mathbf{z})$ and the excited neuron $j, \sigma(n) = \sigma_0 \exp\left(-n/\tau_1\right)$, and $\eta(n) = \eta_0 \exp\left(-n/\tau_2\right)$. The learning is stopped when no noticeable change in the weight vectors is observed. Thereafter, the winning neuron with the best similarity between its weight vector and the WPT feature is identified, and the two-dimensional coordinates of the winning neuron are the components of the projected feature.

A PCA and NLDA project the WPT features into the eight-dimensional subspaces in the same way as an LDA. However, in the case of an SOFM, the output layer is defined as a 100×100 two-dimensional lattice. When the learning procedure of each projection method was completed, the test dataset was applied to the four projection methods.

B. Visualization and Quantitative Comparison

The projection results for the test dataset were first evaluated for one subject. Fig. 3 shows the reduced features when using: 1) an LDA; 2) PCA; 3) NLDA; and 4) SOFM. For the LDA and NLDA, the different class features were well separated, as both methods used supervised learning criteria. In contrast, the clusters of features in the PCA plot were overlapped, as the PCA performed an orthogonal projection to retain the variance of all features. Although the SOFM effectively clustered the features belonging to the same class, some features were mis-clustered with a large distance from the desired cluster. This was because

TABLE I
AVERAGE VALUES OF SAMMON'S STRESS AND FISHER'S INDEX

	LDA	PCA	NLDA	SOFM
Sammon's stress, E	0.9764	0.3548	0.9816	0.9827
Fisher's index, J	25345.8	0.0839	5248.8	47.2026

TABLE II
AVERAGE VALUES OF MLP CLASSIFICATION SUCCESS RATE AND PROCESSING TIME

	LDA	PCA	NLDA	SOFM
success rate [%]	97.4	95.9	97.9	96.2
processing time [msec]	2	2	150	300

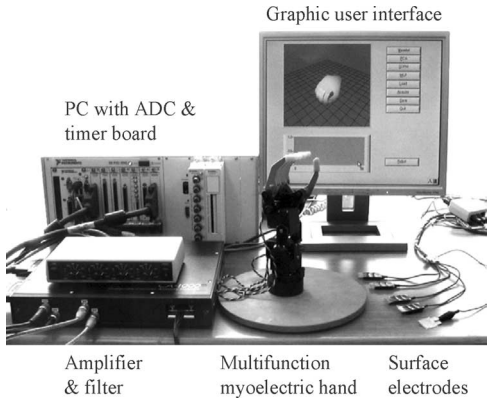

Fig. 4. Experimental setup.

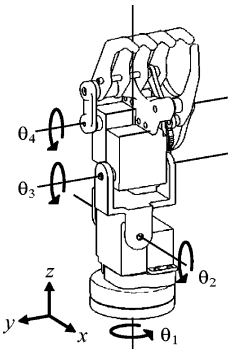

Fig. 5. Multifunction myoelectric hand with four DOFs.

the SOFM nonlinearly transformed the WPT features without any class information.

Sammon's stress [26] is a measure of how much the interpattern distances are changed when the patterns are projected from the original feature space to a reduced feature space. Sammon's stress is defined as

$$E = \frac{\sum_{\mu=1}^{m-1}\sum_{\nu=\mu+1}^{m}[d^*(\mu,\nu)-d(\mu,\nu)]^2/[d^*(\mu,\nu)]}{\sum_{\mu=1}^{m-1}\sum_{\nu=\mu+1}^{m}d^*(\mu,\nu)} \quad (10)$$

where $d^*(\mu,\nu)$ and $d(\mu,\nu)$ are the distances between pattern μ and pattern ν in the original feature space to the reduced feature space, respectively. Meanwhile, Fisher's index is a measure of the class separability of the projected features, and is defined as

$$J = \frac{\det\left(\tilde{\mathbf{S}}_B\right)}{\det\left(\tilde{\mathbf{S}}_W\right)} \quad (11)$$

where $\tilde{\mathbf{S}}_B$ and $\tilde{\mathbf{S}}_W$ are the between-class scatter matrix and within-class scatter matrix in the projected space, respectively. The projections were performed by using a test dataset from ten subjects. Table I shows the average Sammon's stress and Fisher's index values for the four projection methods. Although the LDA was a linear projection, it generated a large Sammon's stress value, similar to those for the NLDA and SOFM. This was because the LDA projected the features onto nonorthogonal principal vectors to maximize the class separability. For Fisher's index, the LDA clearly produced the best performance, and the supervised methods were evidently superior to the unsupervised methods as regards class separability.

The projected features were applied to the MLP classifier, and classifications performed by using the test dataset for ten subjects. At the same time, the processing time for the four projection methods was also monitored. The experiments were executed on a 1.8 GHz Pentium IV PC. Table II shows the average values of the MLP classification success rate and processing time for the four projection methods. The NLDA and LDA both had a higher success rate than that of the PCA and SOFM. This result was also consistent with the comparative results of the class separability. However, the NLDA and SOFM required much more processing time, due to the nonlinear computations for the high-dimensional features. To implement real-time pattern recognition, the processing time should be less than the window increment, 125 ms, making the NLDA and SOFM inadequate for real-time processing. Accordingly, these results show that the LDA produced a better performance for the class separability, and the LDA-projected features improved the classification accuracy. In addition, the short processing time of an LDA makes it suitable for real-time EMG pattern recognition.

V. MULTIFUNCTION MYOELECTRIC HAND CONTROL

The proposed method was used to implement a real-time EMG pattern-recognition system for a multifunction myoelectric hand developed in this study. Fig. 4 shows the experimental setup, including four surface electrodes, an amplifier and filter system, PC with A/D converter and timer board, graphic user interface, and multifunction myoelectric hand.

As shown in Fig. 5, the developed hand had four DOFs, including pronation and supination (θ_1), radial flexion and ulnar flexion (θ_2), wrist flexion and extension (θ_3), and hand open and grasp (θ_4). The total length and weight of the hand were 200 mm and 790 g, respectively. Each joint was actuated by an *RC*-servo motor (HSR-5995TG, HITEC), including an embedded position controller with potentiometer feedback.

The control commands were given by a 20 ms cycle pulse train with variable duty rates. Plus, a timer board (6601, NI) was used to generate the pulse train.

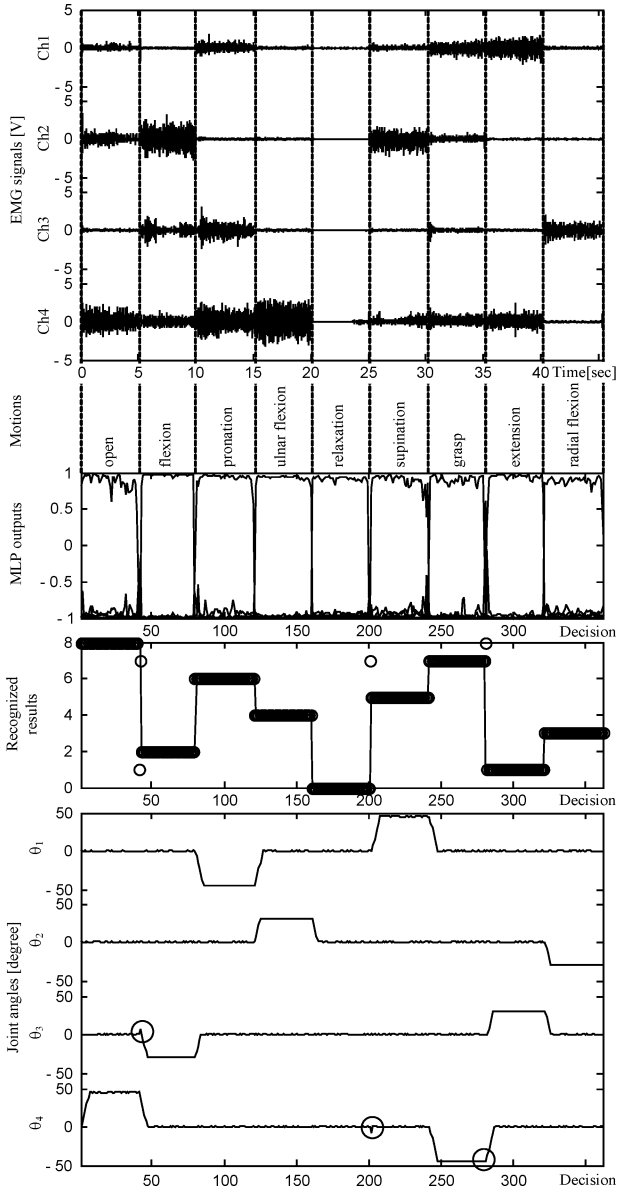

Fig. 6. Four-channel EMG signals, recognized results, and joint angles.

Fig. 6 shows the four-channel EMG signals, MLP outputs, recognized results, and joint angles. The EMG signals were typical data recorded from a typical subject. The subject performed nine hand motions, and each motion was switched to another in random order. The MLP had nine output values from -1.0 to 1.0. The maximum output was selected as the recognized motion in every decision. In the recognized results, each motion was assigned a number from 0 to 8. A solid line and open circle were used to denote the desired output and recognized motion, respectively. The results were stable for steady-state motions, with the exception of transient-state motions. In the experiment, the proposed method achieved a correct classification accuracy of as high as 97.4%. This result was consistent with the results from the offline experiment in the previous section. To control the multifunction myoelectric hand, reference joint angles were predetermined corresponding to the nine hand motions in steady states. In addition, to realize hand motions similar to those of a human in a transient state, the change in the reference joint angle was limited to $\pm$ 7.5° for every decision. The bottom of Fig. 6 shows the actual joint angles controlled by the position controllers for the *RC*-servo motors. The several position errors, marked with circles, were due to incorrect recognition at the beginning and ending of the motions. However, these position errors were reduced by ensuring correct recognitions. Fig. 7 shows the multifunction myoelectric hand controlled by EMG signals. In this figure, the dashed lines indicate the directions of the motions, and the myoelectric hand shows the posture in a steady state.

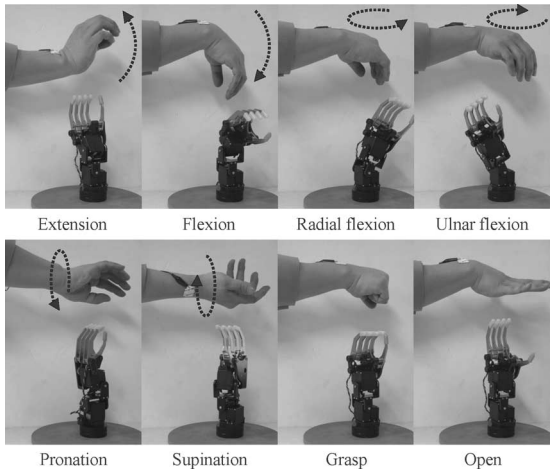

Fig. 7. Myoelectric hand controlled by real-time EMG pattern recognition.

As an example, the recognition procedure for pronation is explained. In the case of pronation, stronger EMG signals were measured in channels 1, 3, and 4 compared to channel 2. Fig. 8 shows the EMG signals in the transient state from flexion to pronation. The MLP outputs are shown in the middle of Fig. 8. The square and circle denote the outputs of the MLP assigned to a flexion and pronation, respectively. These outputs were generated every 125 ms. This interval was the same as the increment of the data window. First, the subject's intention to perform a pronation was given at time t_1. However, the pronation could not be recognized at time t_a, as the pattern recognition was performed by using the data sampled from the previous step not including time t_1. After 125 ms, the data window was increased, and the pronation was correctly recognized at time t_b. Since the control commands were generated by using a timer board, about 40 ms of processing time was needed to modulate the duty rate of the pulse train. Therefore, the control command for pronation was given at time t_2, as shown in the bottom of Fig. 8. During a transient state, the reference joint angle changed with a decrement of $-7.5°$ every 125 ms. Therefore, the actual joint angle decreased from 0 to $-45°$ during 750 ms. Table III shows that the total processing time was 97 ms, less than the window increment of 125 ms. Therefore, the operation delay was less than 300 ms, making the proposed method applicable to the control of a multifunction myoelectric hand.

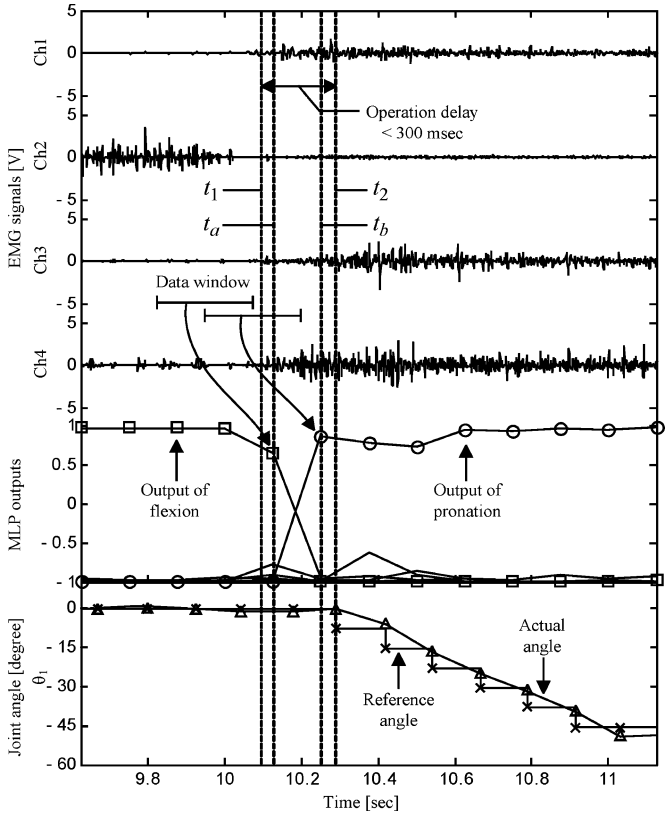

Fig. 8. Transient state from flexion to pronation.

TABLE III
AVERAGE PROCESSING TIME FOR REAL-TIME PATTERN RECOGNITION

Processes	Processing time [msec]
Wavelet packer transform	30
Linear discriminant Analysis	2
Multilayer perceptron	5
Myoelectric hand control	40
Others	20
Total processes	97

VI. CONCLUSION

This paper proposed a real-time EMG pattern-recognition system for multifunction myoelectric hand control. The system is composed of a WPT, LDA, and MLP. To recognize nine kinds of hand motion from four-channel EMG signals, the features are first extracted by using a WPT. Thereafter, an LDA is used for linear supervised feature projection to reduce the dimensionality of the WPT features and improve the class separability. Finally, the LDA-projected features are applied to an MLP. From a visualization and quantitative comparison, the LDA projection produced a better class separability, while the LDA-projected features improved the classification accuracy with a short processing time. By using the proposed method, a real-time EMG pattern-recognition system was implemented for a multifunction myoelectric hand developed in this study. The experimental results confirmed that the proposed method achieved a high recognition accuracy, and the subject could control the myoelectric hand without any perceived operation time delay.

In this paper, it was assumed that EMG signals result from a static contraction in a steady-state motion and fixed movement velocity in a transient-state motion. Consequently, this makes it difficult to apply the proposed method to the tasks of daily living for a limb-deficient individual. Accordingly, future work will investigate using the proposed method to recognize hand motions from EMG signals related to dynamic contractions and various movement velocities.

REFERENCES

[1] *MYOBOCK Arm Components*. OttoBock HealthCare, Duderstadt, Germany, 2005.
[2] S. C. Jacobson, D. F. Knutti, R. T. Johnson, and H. H. Shears, "Development of the Utah artificial arm," *IEEE Trans. Biomed. Eng.*, vol. BME-29, no. 4, pp. 249–269, Apr. 1982.
[3] P. J. Kyberd, O. E. Holland, P. H. Chappel, S. Smith, R. Tregidgoi, P. J. Bagwell, and M. Snaith, "MARCUS: A two degree of freedom hand prosthesis with hierarchical grip control," *IEEE Trans. Rehabil. Eng.*, vol. 3, no. 1, pp. 70–76, Mar. 1995.
[4] C. M. Light and P. H. Chappell, "Development of a lightweight and adaptable multiple-axis hand prosthesis," *Med. Eng. Phys.*, vol. 22, pp. 679–684, 2000.
[5] J. Butterfab, M. Grebenstein, H. Liu, and G. Hirzinger, "DLR-hand II: Next generation of a dexterous robot hand," in *Proc. IEEE Int. Conf. Robot. Autom.*, 2001, pp. 109–114.
[6] B. Hudgins, P. A. Parker, and R. N. Scott, "A new strategy for multifunction myoelectric control," *IEEE Trans. Biomed. Eng.*, vol. 40, no. 1, pp. 82–94, Jan. 1993.
[7] F. H. Y. Chan, Y. S. Yang, F. K. Lam, Y. T. Zhang, and P. A. Parker, "Fuzzy EMG classification for prosthesis control," *IEEE Trans. Rehabil. Eng.*, vol. 8, no. 3, pp. 305–311, Sep. 2000.
[8] H. P. Huang, Y. H. Liu, L. W. Liu, and C. S. Wong, "EMG classification for prehensile posture using cascaded architecture of neural networks with self-organizing maps," in *Proc. IEEE Int. Conf. Robot. Autom.*, Sep. 2003, pp. 1497–1502.
[9] K. Englehart and B. Hudgins, "A robust, real-time control scheme for multifunction myoelectric control," *IEEE Trans. Biomed. Eng.*, vol. 50, no. 7, pp. 848–854, Jul. 2003.
[10] Y. Huang, K. B. Englehart, B. Hudgins, and A. D. C. Chan, "Optimized Gaussian mixture models for upper limb motion classification," in *Proc. IEEE Int. Conf. EMBS*, Sep. 2004, pp. 72–75.
[11] A. D. C. Chan and K. B. Engelehart, "Continuous myoelectric control for powered prostheses using hidden Markov models," *IEEE Trans. Biomed. Eng.*, vol. 52, no. 1, pp. 121–124, Jan. 2005.
[12] B. Karlik, M. O. Tokhi, and M. Alci, "A fuzzy clustering neural network architecture for multifunction upper-limb prosthesis," *IEEE Trans. Biomed. Eng.*, vol. 50, no. 11, pp. 1255–1261, Nov. 2003.
[13] A. Hiraiwa, N. Uchida, N. Sonehara, and K. Shimohara, "EMG pattern recognition by neural networks for prosthetic fingers control—Cyber finger," in *Proc. Int. Symp. Meas. Control Robot.*, Nov. 1992, pp. 535–542.
[14] S. H. Park and S. P. Lee, "EMG pattern recognition based on artificial intelligence techniques," *IEEE Trans. Rehabil. Eng.*, vol. 6, no. 4, pp. 400–405, Dec. 1998.
[15] K. Englehart, B. Hudgins, P. A. Parker, and M. Stevenson, "Classification of the myoelectric signal using time–frequency based representations," *Med. Eng. Phys.*, vol. 21, pp. 431–438, 1999.
[16] K. Englehart, B. Hudgins, and P. A. Parker, "A wavelet-based continuous classification scheme for multifunction myoelectric control," *IEEE Trans. Biomed. Eng.*, vol. 48, no. 3, pp. 302–311, Mar. 2001.
[17] D. Nishikawa, W. Yu, H. Yokoi, and Y. Kakazu, "EMG prosthetic hand controller discriminating ten motions using real-time learning method," in *Proc. IEEE/RSJ Int. Conf. Intell. Robot. Syst.*, 1999, pp. 1592–1597.
[18] O. Fukuda, T. Tsuji, M. Kaneko, and A. Otuka, "A human-assisting manipulator teleoperated by EMG signals and arm motions," *IEEE Trans. Robot. Autom.*, vol. 19, no. 2, pp. 210–222, Apr. 2003.
[19] *Surface Electromyography: Detection and Recording*. Delsys Inc., Boston, MA, 2002.

[20] N. Saito and R. R. Coifman, "Local discriminant bases and their applications," *J. Math. Imag. Vis.*, vol. 5, no. 4, pp. 337–358, 1995.
[21] S. G. Mallat, "A theory for multiresolution signal decomposition: The wavelet representation," *IEEE Trans. Pattern Anal. Mach. Intell.*, vol. 11, no. 7, pp. 674–693, Jul. 1989.
[22] C. Chatterjee and V. P. Roychowdhury, "On self-organizing algorithms and networks for class-separability features," *IEEE Trans. Neural Netw.*, vol. 8, no. 3, pp. 663–678, May 1997.
[23] R. O. Duda, P. E. Hart, and D. G. Stork, *Pattern Classification*. New York: Wiley, 2001.
[24] D. Lowe and R. Webb, "Optimized feature extraction and Bayes decision in feed-forward classifier networks," *IEEE Trans. Pattern Anal. Mach. Intell.*, vol. 13, no. 4, pp. 355–364, Apr. 1991.
[25] T. Kohonen, "The self-organizing map," *Proc. IEEE*, vol. 78, no. 9, pp. 1464–1480, Sep. 1990.
[26] J. W. Sammon, "A nonlinear mapping for data structure analysis," *IEEE Trans. Comput.*, vol. C-18, no. 5, pp. 401–409, May 1969.

Jun-Uk Chu (M'05) received the B.S. degree in electrical engineering from Yeungnam University, Gyeongsan, Korea, in 1998, and the M.S. degree in electronic engineering in 2000 from Kyungpook National University, Daegu, Korea, where he is currently working toward the Ph.D. degree in electronic engineering.

From 2002 to 2006, he was a Research Scientist with the Korea Orthopedics and Rehabilitation Engineering Center, Incheon, Korea. His current research interests include biosignal processing, pattern recognition, machine learning, and intelligent control.

Inhyuk Moon (M'99) received the B.E. and M.E. degrees in electronics engineering from Gyeongsang National University, Jinju, Korea, in 1992 and 1994, respectively, and the Ph.D. degree in computer-controlled mechanical systems from Osaka University, Suita, Japan, in 1998.

During 1999, he was a Postdoctoral Researcher with the Organization of Hamamatsu Technopolis, Shizuoka, Japan. From 2000 to 2002, he was a Research Professor with the Department of Biomedical Engineering, Yonsei University, Wonju, Korea. From 2002 to 2005, he was the Korea Orthopedics and Rehabilitation Engineering Center, Incheon, Korea. In 2005, he joined the Department of Mechatronics Engineering, Dong-Eui University, Busan, Korea, where he is currently an Assistant Professor. His current research interests include pattern recognition, rehabilitation robotics, and biomechatronic engineering.

Yun-Jung Lee (M'90) received the B.S. degree in electronic engineering from Hanyang University, Seoul, Korea, in 1984, and the M.S. and Ph.D. degrees in electrical engineering from the Korea Advanced Institute of Science and Technology, Daejon, Korea, in 1986 and 1994, respectively.

From 1986 to 1989, he was a Researcher with the Korea Institute of Machinery and Metals. During 1999, he was a Visiting Scholar at the Hirose and Yoneda Laboratory, Department of Mechano-Aerospace Engineering, Tokyo Institute of Technology, Tokyo, Japan. Since 1995, he has been with Kyungpook National University, Daegu, Korea, where he is currently an Associate Professor with the School of Electrical Engineering and Computer Science. His current research interests include multilegged robots, service robots, intelligent control, and embedded systems.

Shin-Ki Kim received the B.S. M.S., and Ph.D. degrees in mechanical engineering from Kyunghee University, Seoul, Korea, in 1988, 1990, and 2001, respectively.

From 1990 to 1995, he was a Research Scientist with LG Precision Company, Ltd. Since 1995, he has been a Principal Research Scientist with the Korea Orthopedics and Rehabilitation Engineering Center, Incheon, Korea. His current research interests include biomechanics, rehabilitation systems, assistive products, and orthopedic implants.

Mu-Seong Mun received the B.S. and M.S. degrees in mechanical system design from Seoul National University, Seoul, Korea, in 1978 and 1982, respectively, and the Ph.D. degree in biomedical engineering from the University of Minnesota, Minneapolis, in 1992.

From 1993 to 1994, he was a Research Professor with the Department of Orthopedic Surgery, Kyunghee University. Since 1994, he has been the Director of the Korea Orthopedics and Rehabilitation Engineering Center, Incheon, Korea. His current research interests include rehabilitation systems, assistive products, and orthopedic implants.